Noname manuscript No.
(will be inserted by the editor)

Use of Flip Ambiguity Probabilities in Robust Sensor Network Localization

Anushiya A Kannan · Barış Fidan · Guoqiang Mao

Received: date / Accepted: date

Abstract Collinear or near collinear placement of some sensors in a wireless sensor network causes the location estimates of nearby sensors to be sensitive to erroneous

The work was supported by National ICT Australia-NICTA. NICTA is funded by the Australian Government as represented by the Department of Broadband, Communications and the Digital Economy and the Australian Research Council through the ICT Centre of Excellence program.

Anushiya A Kannan

School of Electrical and Information Engineering, University of Sydney, NSW 2006, Australia.

Tel.: +61-2-88122431

Fax: +61-2-88122431

E-mail: anushiya@ee.usyd.edu.au

Barış Fidan

University of Waterloo, Ontario, Canada

E-mail: fidan@uwaterloo.ca

Guoqiang Mao

The University of Sydney and National ICT Australia

E-mail: Guoqiang.Mao@nicta.com.au

distance measurements which leads to large location estimation errors. These errors and the possible propagation of these errors to the entire network or a large portion of it, thereby causing larger estimation errors for some sensors' locations, is a major problem in localization. This phenomenon is well described in rigid graph theory, using the notion of "flip ambiguity". This paper considers arbitrary sensor neighborhoods of two dimensional sensor networks and formulates an analytical expression for the probability of occurrence of the flip ambiguity. Based on the derived probability expression, a methodology is proposed to make the localization algorithms robust by calculating such flip ambiguity probabilities and eliminating potentially poor location estimates as well as assigning confidence factors to the estimated locations to prevent them from ruining the subsequent localization steps. The efficiency of the proposed methodology is demonstrated via a set of simulations.

Keywords Flip Ambiguities · Robust Localization

1 Introduction

Distance based sensor network localization schemes estimate the locations of sensors using inter-sensor distance measurements, which may contain noises, and the a priori known locations of a specific subset of sensors, often termed as anchors. Rigid graph theory [1–5] is a useful framework for analyzing the characteristics of such schemes, which represents the sensor network by an underlying graph $G = (V, E)$ with vertex set V and edge set E, and uniquely associates each sensor s_X with a vertex $X \in V$ and each sensor pair (s_X, s_Y) with known inter-sensor distance with an edge $(X, Y) \in E$. A 2- dimensional representation of the underlying graph $G = (V, E)$ is a mapping $\overline{p} : V \rightarrow \mathcal{R}^2$, which assigns a location in $\mathcal{R}^2$ to each vertex in V, where $\|\overline{p}(X) - \overline{p}(Y)\|$ denotes

the distance between the two locations $\overline{p}(X)$, $\overline{p}(Y)$ of the vertices $X, Y \in V$. The pair $(G, \overline{p})$ representing a given underlying graph $G = (V, E)$ and the representation $\overline{p}$ is called a 2-dimensional *framework*.

A necessary and sufficient condition for unique localization of a sensor network modeled as above is *global rigidity* [1,5]. A framework $(G, \overline{p})$ is globally rigid if every framework $(G, \overline{p}_1)$ satisfying $\|\overline{p}(X) - \overline{p}(Y)\| = \|\overline{p}_1(X) - \overline{p}_1(Y)\|$ for any vertex pair $X, Y \in V$ where $(X, Y) \in E$ also satisfies the same equality for any other vertex pairs that are not connected by a single edge. A relaxed form of global rigidity is rigidity: A framework $(G, \overline{p})$ is rigid if there exists a sufficiently small positive constant ϵ such that every framework $(G, \overline{p}_1)$ satisfying (i) $\|\overline{p}(X) - \overline{p}_1(X)\| < \epsilon$ for all $X \in V$ and (ii) $\|\overline{p}(X) - \overline{p}(Y)\| = \|\overline{p}_1(X) - \overline{p}_1(Y)\|$ for any vertex pair $X, Y \in V$, which are connected by an edge in E, also satisfies the equality in (ii) for any other vertex pairs that are not connected by a single edge.

In order to have a finite number of solutions, rigidity is needed. A rigid framework $(G, \overline{p})$ without global rigidity may suffer from *flip* and *discontinuous flex ambiguities*, making the representation of G inconsistent with $\overline{p}$, in the sense that it differs from other such representations at most by translation, rotation or reflection [3,4]. *This paper only focuses on flip ambiguities.* Flip ambiguity occurs when a vertex (sensor) X of a rigid but not globally rigid underlying graph is reflected across a set of collinear neighbors with the possibility of forming a mirror without violating any distance constraints as shown in Fig. 1(a).

For a globally rigid underlying graph, depending on sensitivity of the *near collinear* neighborhood to the corresponding distance measurement errors, such a reflection of a vertex (sensor) X can still occur across its *near collinear* neighborhood [5] as shown in Fig. 1(b).

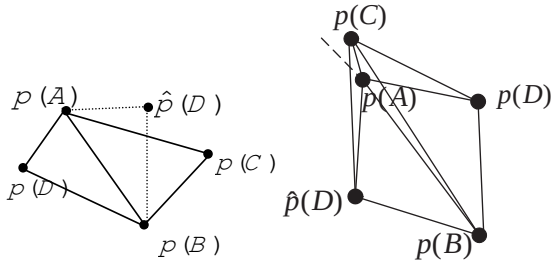

(a) (b)

Fig. 1 Flip ambiguity: Reflecting $p(D)$ through a mirror formed by neighbors, a new realization $\hat{p}(D)$ is obtained without violating the distance constraints. (a) Flip ambiguity in rigid but not globally rigid underlying graph. (b) Flip ambiguity in globally rigid underlying graph due to the *near collinear* neighborhood and its sensitivity to the corresponding distance measurement errors.

An empirical study in [6] demonstrates that increasing the number of known neighbors in a neighborhood is able to reduce but not fully eliminate flip ambiguities. Moreover, anchors are the only location known neighbors at the initial iteration of a localization algorithm [4, 7–14] and are limited in number due to the associated cost, causing more frequent occurrences of flip ambiguities at the early iterations. The usage of these erroneous location estimates may continue to degrade the location estimates of the subsequent iterations [6], and propagate in an avalanche fashion for several iterations affecting the location estimates of either the entire network, or a large portion of it. Many localization algorithms in the literature, including both centralized and distributed algorithms, show the traces of this avalanche error propagation behavior one of which is shown in Fig. 2.

Almost collinear placement of the three anchors marked as anchor 1, 2 and 3 in Fig. 2 causes a large number of sensors (shown within the rectangle in Fig. 2), which may not necessarily be the one-hop neighbors of these three anchors, to be flipped to incorrect

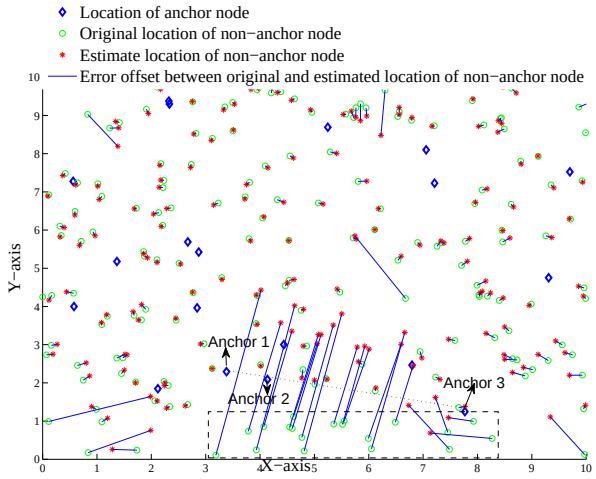

Fig. 2 Avalanche error propagation of flip ambiguity seen in a centralized localization algorithm presented in [15], [16].

positions. A detailed description of flip ambiguities and the resulting avalanche error propagation effects are presented in [6, 16].

Flip ambiguities do not necessarily occur in every sensor network, but when they occur, the performance of localization can be significantly degraded as shown in Fig. 2. Thus, identification and mitigation of flip ambiguities is essential in improving the reliability of the sensor network localization algorithm.

This paper derives an analytical equation for the probability of flip ambiguities of arbitrary sensor neighborhoods. The significance of this derivation is two folds: (i) The derived probability expression can be used for stochastic analysis of localization processes that are affected by flip ambiguities, such as the ones mentioned above. (ii) This expression can be used, as a filtering tool integrated with the localization algorithm, to identify neighborhoods with higher probabilities of flip ambiguity than a predefined threshold value, and eliminate them from being used in the localization process. The integration can be done for both centralized and distributed distance

based localization algorithms to improve the accuracy and reliability of their location estimates. This paper **chooses** to focuss on the performance of distributed sequential localization algorithms as an example [7–11].

The calculated probability of flip ambiguity may also be used in assigning confidence factors to the location estimates such that estimates obtained using a neighborhood with a larger probability of flip ambiguity will have a lower confidence factor and vice versa. Confidence factor assignment and its usage are beyond the scope of this paper. We refer interested readers to [17] and references therein for detailed discussion on the topic.

The rest of the paper is organized as follows: Section 2 presents the recent relevant works. Section 3 formulates the problem by analyzing the effects of distance measurement errors on flip ambiguities. Section 4 derives an analytical equation for the probability of flip ambiguity. Analytical probabilities are compared against simulated counterparts in Section 5. Section 6 presents an analysis of substantial and negligible flip ambiguities. Section 7 demonstrates the performance enhancement by the usage of probability of flip ambiguities in sequential localization algorithm. This paper is concluded in Section 8, together with intended future work.

2 Related Work

The researchers have approached the flip ambiguity problem in a number of different perspectives in the literature. The studies in [1, 2, 18, 19] explored the underlying representative graph structure of the sensor network. The work in [1, 2] claimed that maintaining a global rigidity in the networks is a way of mitigating flip ambiguities from the localization algorithms in those networks. Global rigidity is however a suffi-

cient condition for unique localization which is often met only in a denser network. In some underlying graph structures, the need for global rigidity may be compensated by a priori information [5].

The algorithm in [18] approached the problem of flip ambiguity in two steps. This algorithm firstly identified the sensors at the boundary using the boundary detection algorithms in the literature and mitigated flip ambiguities in their location estimates using the principle of Voronoi diagram and Delaunay graph. Then the algorithm used the boundary sensors as anchors to mitigate flip ambiguities from rest of the network localization. The study by the same authors in [20] replaced the need for the boundary detection algorithm by an incremental landmark selection algorithm, which selects landmarks incrementally in a distributed manner until the global rigidity property of the Delaunay graph and the coverage property of not being far from the embedded Delaunay complex are met.

It is non-trivial to design an efficient distributed algorithm for testing global rigidity as neither rigidity nor connectivity can be tested locally by nature [21]. The distributed nature and the easily implementable characteristic of trilateration [4, 7, 8, 12, 22, 23] makes it an attractive choice of localization method. The study in [21] pointed out that only a subset of localizable sensors with globally rigid underlying graphs are localized using trilateration. This study also noted trilateration as a special case of wheel graphs, a globally rigid graph structure, and claimed that using wheel graphs in localization algorithms instead may improve the number of localized nodes.

The theory of graph realization does not account for inter-sensor measurement errors of real applications [22]. The algorithms in [19, 24] recorded all possible location estimates of sensors during the localization process and eliminated the incompatible estimates whenever possible, which is computationally not practical.

Localization algorithms in [4, 6, 16, 22, 23] identified possible flip ambiguities and took necessary actions to mitigate them from the localization process. These algorithms considered a quadruple of sensors s_A, s_B, s_C, s_D with known locations $p(A)$, $p(B)$, $p(C)$ and inter-sensor distance measurements $\overline{d}_{AD}$, $\overline{d}_{BD}$, $\overline{d}_{CD}$ from sensors s_A, s_B, s_C to sensor s_D as a *fully connected sensor quadruple*. They formulated robustness criteria to identify possible flip ambiguities in the location estimate of sensor s_D with respect to the ordered sensor quadruple $s_A s_B s_C s_D$. Only those sensor quadruples that are identified as robust (not suffering from possible flip ambiguities) are then used in the localization process.

The work in [4] formulated the robustness criterion to identify possible flip ambiguities in fully connected sensor quadruples based on the following generic localization method:

Step 1. Use distance measurements $\overline{d}_{AD}$, $\overline{d}_{BD}$ together with known locations $p(A)$, $p(B)$ to find the two possible locations $\hat{p}(D)$ and $\hat{p}'(D)$ of sensor s_D as intersection points of the circles $\mathcal{C}(p(A), \overline{d}_{AD})$ with center $p(A)$ and radius $\overline{d}_{AD}$ and $\mathcal{C}(p(B), \overline{d}_{BD})$ with center $p(B)$ and radius $\overline{d}_{BD}$. Note: locations $\hat{p}(D)$ and $\hat{p}'(D)$ are symmetrical across the line joining the points $p(A)$ and $p(B)$.

Step 2. Use distance measurement $\overline{d}_{CD}$ together with known location $p(C)$ to decide on which of $\hat{p}(D)$ and $\hat{p}'(D)$ to choose as the location estimate of sensor s_D satisfying the distance constraints.

It was noted in [6,22] that [4] chose information from sensors s_A, s_B in the first step and used the information from sensor s_C in the second step. If instead, information from sensors s_A, s_C are chosen in the first step and the information from sensor s_B is used in the second step, it may result in a different value of the robustness criterion

and may affect localization performance. Such dependency is eliminated in [6, 22] by including all three permutation (s_A, s_B, s_C), (s_A, s_C, s_B) and (s_B, s_C, s_A) as the order of choice of the neighbors in the corresponding robustness criterion.

The study in [23] provided a formal geometric analysis of flip ambiguity problem using similar notions as those in [4,22]. It developed a generic formal method for quantifying the likelihood of flip ambiguities for arbitrary sensor neighborhood geometries. Specifically, for a fully connected sensor quadruple $s_A s_B s_C s_D$ with known node locations s_A and s_B, a possible region for the location of s_C is determined such that the sensor s_D can be uniquely localized. Thus, in an arbitrary sensor neighborhood $s_A s_B s_C$, for any pair of anchors s_A and s_B, if the location of the third anchor s_C is not contained within the possible region identified for the location of s_C, then the location estimate of the sensor s_D in the fully connected sensor quadruple $s_A s_B s_C s_D$ is tagged as likely to have flip ambiguity.

The analysis in [4, 22, 23] has been conducted under the assumption of unknown sensor s_D having access to inter sensor distance measurement from all three of its neighbors, where, only one distance measurement used in Step 2 is considered to be erroneous while the other two distance measurements used in Step 1 are considered accurate.

In contrast to studies in [4,22] and [23] which considered unique localizability with only one erroneous distance measurement while the other two distance measurements are considered accurate, references [6, 16] accommodated the errors in one or more inter-sensor distance measurements and established a robustness criterion to identify possible flip ambiguities. References [6,16] enhanced the performance of previous works by noting that the two possible location estimates $\hat{p}(D)$ and $\hat{p}'(D)$ of sensor s_D obtained in Step 1 are in fact inside two intersection regions of the annul: $\mathcal{R}(s_A, \overline{d}_{AD}+\overline{\epsilon}, \overline{d}_{AD}-\overline{\epsilon})$

and $\mathcal{R}(s_B, \overline{d}_{BD} + \overline{\epsilon}, \overline{d}_{BD} - \overline{\epsilon})$ rather than at the two intersection points of the circles $\mathcal{C}(s_A, \overline{d}_{AD})$ and $\mathcal{C}(s_B, \overline{d}_{BD})$ where $\overline{\epsilon}$ represents an error bound in distance measurement errors, $\mathcal{C}(s_X, \overline{d}_{XD})$ denotes the circle with center s_X and radius $\overline{d}_{XD}$ and $\mathcal{R}(s_X, \overline{d}_{XD} + \overline{\epsilon}, \overline{d}_{XD} - \overline{\epsilon})$ denotes the annulus in between $\mathcal{C}(s_X, \overline{d}_{XD} + \overline{\epsilon})$ and $\mathcal{C}(s_X, \overline{d}_{XD} - \overline{\epsilon})$ for $X \in \{A, B\}$. It is worth noting here that, this analysis still maintain the assumption of symmetry in its analysis by only considering point pairs $\hat{p}(D)$ and $\hat{p}'(D)$ where $\hat{p}(D)$ is in one intersection region of the annul and $\hat{p}'(D)$ is a symmetrical point in the other intersection region of the annul, where the intersection regions are symmetrical to the line connecting $p(A)$ and $p(B)$. The analysis did not let the points $\hat{p}(D)$ and $\hat{p}'(D)$ move independently inside the intersection regions of the annul independently in order to find the best location estimate.

The assumption of true location and the possible flipped location are symmetrical with respect to a pair of neighboring nodes may however cause false alarms in the identification of possible flip ambiguities. In this paper, this assumption of symmetry is removed by independently considering all possible locations $\hat{p}(D)$ and $\hat{p}'(D)$ within the corresponding intersections of the annul without considering any relationship between the two locations $\hat{p}(D)$ and $\hat{p}'(D)$ and an analytical equation for the probability of flip ambiguity for a given neighborhood is defined. This paper also enhances the performance of the recent study by the co-authors in [6, 16] by replacing the need of making a binary decision of accepting or rejecting a neighborhood made by the robustness criterion with a soft decision based on the probabilities of flip ambiguities in arbitrary sensor neighborhoods. The derived flip ambiguity probability can be applied to identify neighborhoods having higher probabilities of flip ambiguity than a predefined threshold value, and eliminate these neighborhoods from being used in the localisation process. The same flip ambiguity probability may also be used in assigning confidence factors to

the location estimates such that estimates obtained using a neighborhood with larger probability of flip ambiguity have a lower confidence factor and vice versa.

All the techniques presented in this related work and this paper aims to achieve good mitigation of flip ambiguity in each location estimate and consider the estimated locations are accurate when iteratively proceed to localize the location unknown nodes. But if flip ambiguity was not mitigated efficiently at any step of the localisation process, it is possible to have an avalanche error propagation as explained in Section 1.

3 Problem Formulation

In this section, the probability of flip ambiguity is formulated for sensor neighborhoods in the form of fully connected quadrilaterals (FCQs), quadruple of sensors all of which are neighbors of each other, i.e., the distance between any pair is known or measurable. Using the same notations as in Graph theory, for any sensor pair s_X and s_Y in (G, p), $\|p(X) - p(Y)\|$ and $\overline{d}_{XY}$ denote the true and measured distances between sensors s_X and s_Y respectively.

The analysis uses a disc transmission model of radius R around each sensor s_X, where

Assumption 1 *Two sensors s_X, s_Y are said to be neighbors of each other and are able to measure their inter-sensor distance to each other if and only if $\|p(X) - p(Y)\| \leq R$.*

An additive Gaussian distribution with zero mean and a variance σ^2 has been widely used to model the distance measurement errors [25] as

$$\overline{d}_{XY} = \overline{d}_{YX} = \|p(X) - p(Y)\| + \mathcal{N}(0, \sigma^2) \tag{1}$$

and the analysis in this paper uses an additive truncated Gaussian distribution for the inter-sensor distance measurement errors, where

Assumption 2 *For every neighbor node pair s_X and s_Y, the absolute value of the distance measurement error satisfies,*

$$| \, \|p(X) - p(Y)\| - \overline{d}_{XY} | \leq \overline{\epsilon} \tag{2}$$

with certain probability for a given threshold $\overline{\epsilon} > 0$.

For example, the absolute value of the distance measurement error is $\leq 3\sigma$ with a probability of 99% and is $\leq 2\sigma$ with a probability of 66%.

Let $s_A s_B s_C s_D$ be an ordered FCQ with known locations $p(A)$, $p(B)$, $p(C)$ and measured inter-sensor distances $\overline{d}_{AD}$, $\overline{d}_{BD}$ and $\overline{d}_{CD}$. Using Assumption 2, it can be stated that

$$\begin{aligned}
&\overline{d}_{AD} \in [\|p(A) - p(D)\| - \overline{\epsilon}, \|p(A) - p(D)\| + \overline{\epsilon}], \\
&\overline{d}_{BD} \in [\|p(B) - p(D)\| - \overline{\epsilon}, \|p(B) - p(D)\| + \overline{\epsilon}] \text{ and} \\
&\overline{d}_{CD} \in [\|p(C) - p(D)\| - \overline{\epsilon}, \|p(C) - p(D)\| + \overline{\epsilon}]
\end{aligned} \tag{3}$$

or, equivalently,

$$\begin{aligned}
&\|p(A) - p(D)\| \in [\overline{d}_{AD} - \overline{\epsilon}, \overline{d}_{AD} + \overline{\epsilon}], \\
&\|p(B) - p(D)\| \in [\overline{d}_{BD} - \overline{\epsilon}, \overline{d}_{BD} + \overline{\epsilon}] \text{ and} \\
&\|p(C) - p(D)\| \in [\overline{d}_{CD} - \overline{\epsilon}, \overline{d}_{CD} + \overline{\epsilon}]
\end{aligned} \tag{4}$$

Exploiting (4), the following constraint on the estimated location $\hat{p}(D) = (\hat{x}, \hat{y})$ of sensor s_D can be asserted:

$$\hat{p}(D) \in R_D^{ABC}, \text{ where region} \tag{5}$$

$$R_D^{ABC} \triangleq \left\{ p(D) : \begin{cases} | \, \|p(A) - p(D)\| - \overline{d}_{AD} \, | \leq \overline{\epsilon} \text{ and} \\ | \, \|p(B) - p(D)\| - \overline{d}_{BD} \, | \leq \overline{\epsilon} \text{ and} \\ | \, \|p(C) - p(D)\| - \overline{d}_{CD} \, | \leq \overline{\epsilon} \end{cases} \right\}$$

which is formed by the intersection of three rings

$$\begin{aligned} &| \, \|p(A) - p(D)\| - \overline{d}_{AD} \, | \leq \overline{\epsilon}, \\ &| \, \|p(B) - p(D)\| - \overline{d}_{BD} \, | \leq \overline{\epsilon} \ \text{ and} \\ &| \, \|p(C) - p(D)\| - \overline{d}_{CD} \, | \leq \overline{\epsilon} \end{aligned} \tag{6}$$

as shown in Fig. 3(a). Instead, if consideration is given to constraints asserted by only two neighboring sensors s_A and s_B, then the constraints on the estimated location $\hat{p}(D) = (\hat{x}, \hat{y})$ of sensor s_D is given by

$$\hat{p}(D) \in R_D^{AB}, \text{ where region} \tag{7}$$

$$R_D^{AB} \triangleq \left\{ p(D) : \left\{ \begin{array}{l} | \, \|p(A) - p(D)\| - \overline{d}_{AD} \, | \leq \overline{\epsilon} \ \text{ and} \\ | \, \|p(B) - p(D)\| - \overline{d}_{BD} \, | \leq \overline{\epsilon} \end{array} \right. \right\}$$

which is formed by the intersection of two rings

$$\begin{aligned} &| \, \|p(A) - p(D)\| - \overline{d}_{AD} \, | \leq \overline{\epsilon} \text{ and} \\ &| \, \|p(B) - p(D)\| - \overline{d}_{BD} \, | \leq \overline{\epsilon} \end{aligned} \tag{8}$$

The region R_D^{AB} can also be written as (see Fig. 3(b))

$$R_D^{AB} = R_{D_1}^{AB} \cup R_{D_2}^{AB} \tag{9}$$

It can be easily seen from Fig. 3(b) that, by considering constraints imposed only by measured distances from a single neighboring sensor pair (s_A, s_B), the location of sensor s_D can be estimated either in the region $R_{D_1}^{AB}$ or in the region $R_{D_2}^{AB}$ contributing to a possible flip ambiguity with respect to the line AB joining the sensor locations S_A and S_B.

It should be pointed out that the regions $R_{D_1}^{AB}$ and $R_{D_2}^{AB}$ have been shown as disjoint in Fig. 3(b) for simplicity. Depending on the locations $p(A)$ and $p(B)$, the

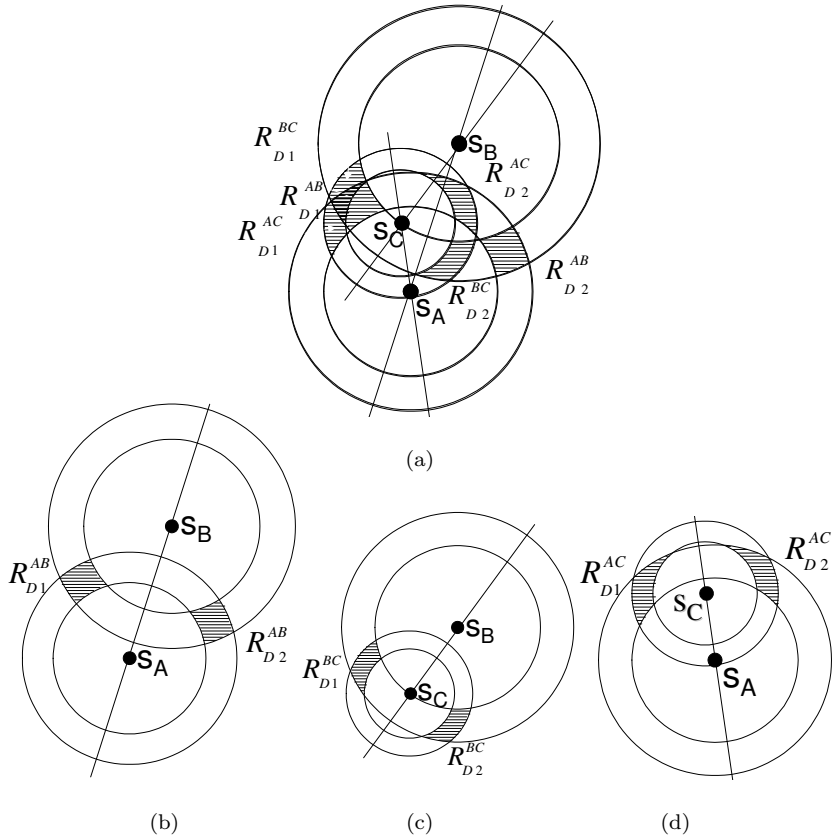

Fig. 3 Possible regions for the location estimate of sensor s_D based on different constraints. (a) Possible region for $\hat{p}(D)$ constrained by measured distances from all three neighbors s_A, s_B and s_C; (b) Possible region for $\hat{p}(D)$ constrained by measured distances from only two neighbors s_A, s_B; (c) Possible region for $\hat{p}(D)$ constrained by measured distances from only two neighbors s_B, s_C; (d) Possible region for $\hat{p}(D)$ constrained by measured distances from only two neighbors s_A, s_C.

corresponding measured distances $\overline{d}_{AD}$, $\overline{d}_{BD}$ and the threshold value $\overline{\epsilon}$, these regions may be joint as illustrated in Fig. 4. In such situations, the boundary separating the two regions $R_{D_1}^{AB}$ and $R_{D_2}^{AB}$ is taken as the line AB joining the sensor locations S_A and S_B.

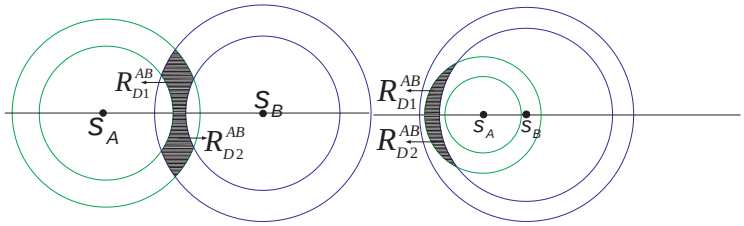

Fig. 4 Examples of possible joint regions $R_{D_1}^{AB}$ and $R_{D_2}^{AB}$.

Similarly, the regions R_D^{AC} and R_D^{BC} can be defined using the constraints imposed by neighboring sensor pairs (s_A, s_C) and (s_B, s_C) respectively (See Fig. 3(c) and (d)) as

$$\begin{aligned} R_D^{AC} &\triangleq \left\{ p(D) : \left\{ \begin{array}{l} \mid \|p(A) - p(D)\| - \overline{d}_{AD} \mid \leq \overline{\epsilon} \text{ and} \\ \mid \|p(C) - p(D)\| - \overline{d}_{CD} \mid \leq \overline{\epsilon} \end{array} \right. \right\} \\ &= R_{D_1}^{AC} \cup R_{D_2}^{AC} \end{aligned} \tag{10}$$

$$\begin{aligned} R_D^{BC} &\triangleq \left\{ p(D) : \left\{ \begin{array}{l} \mid \|p(B) - p(D)\| - \overline{d}_{BD} \mid \leq \overline{\epsilon} \text{ and} \\ \mid \|p(C) - p(D)\| - \overline{d}_{CD} \mid \leq \overline{\epsilon} \end{array} \right. \right\} \\ &= R_{D_1}^{BC} \cup R_{D_2}^{BC} \end{aligned} \tag{11}$$

Using the definitions of the regions R_D^{AB}, R_D^{AC}, R_D^{BC} and Fig. 3, the region R_D^{ABC} in (5) can be written as,

$$\begin{aligned} R_D^{ABC} &= R_D^{AB} \cap R_D^{AC} \cap R_D^{BC} \\ &= (R_{D_1}^{AB} \cup R_{D_2}^{AB}) \cap (R_{D_1}^{AC} \cup R_{D_2}^{AC}) \cap (R_{D_1}^{BC} \cup R_{D_2}^{BC}) \end{aligned} \tag{12}$$

From De-Morgan's rule, R_D^{ABC} can be decomposed into the following eight disjoint regions:

$$R_{D_{p,q,r}}^{ABC} = R_{D_p}^{AB} \cap R_{D_q}^{AC} \cap R_{D_r}^{BC} \; ; \; p, q, r \in \{1, 2\} \tag{13}$$

which can be represented by a Venn diagram as shown in Fig. 5. In this Venn diagram, the regions $R_{D_2}^{AB}$, $R_{D_2}^{AC}$ and $R_{D_2}^{BC}$ are represented by three mutually intersecting discs.

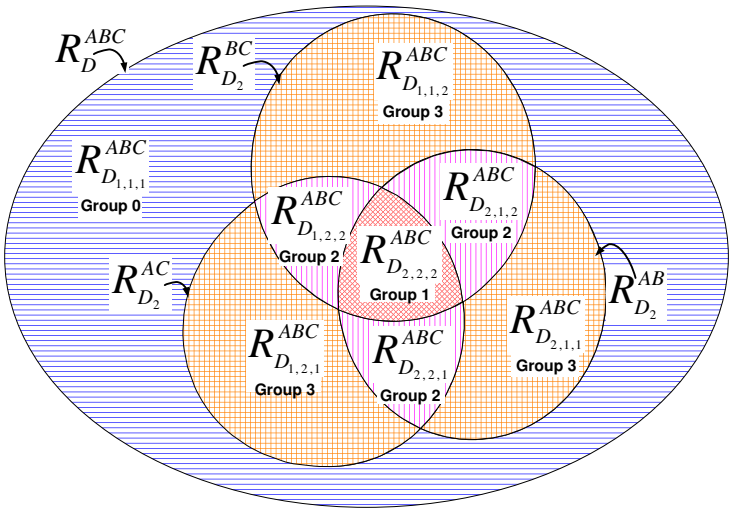

Fig. 5 Venn Diagram representation of (12).

Note that, due to the disjoint nature of the possible eight regions in (13), the true location $p(D)$ of sensor s_D can only be in one of these possible eight regions. Let the regions of intersections $(R_{D_1}^{AB}, R_{D_2}^{AB})$, $(R_{D_1}^{BC}, R_{D_2}^{BC})$ and $(R_{D_1}^{AC}, R_{D_2}^{AC})$ are defined such that

$$\begin{aligned} p(D) &\in R_{D_1}^{AB} \\ p(D) &\in R_{D_1}^{AC} \\ p(D) &\in R_{D_1}^{BC} \end{aligned} \tag{14}$$

giving

$$p(D) \in R_{D_{1,1,1}}^{ABC} = R_{D_1}^{AB} \cap R_{D_1}^{AC} \cap R_{D_1}^{BC} \tag{15}$$

Then, existence of the estimated location $\hat{p}(D)$ in a set represented by any of the three mutually intersecting discs in the Venn diagram corresponds to a flipped realization.

With the help of Fig.5, the possible location estimates can be divided into following four groups.

i) **Group 0:** $\hat{p}(D) \in R^{ABC}_{D_{1,1,1}}$; $p(D)$ and $\hat{p}(D)$ are both in $R^{ABC}_{D_{1,1,1}}$ causing no flip ambiguity.

ii) **Group 1:** $\hat{p}(D) \in R^{ABC}_{D_{2,2,2}}$; $p(D)$ and $\hat{p}(D)$ are in $R^{ABC}_{D_{1,1,1}}$ and $R^{ABC}_{D_{2,2,2}}$ respectively causing possible flip ambiguities with respect to all three lines AB, AC and BC.

iii) **Group 2:** $\hat{p}(D) \in R^{ABC}_{D_{p,q,r}}$ such that p, q, $r \in \{1, 2\}$ and $p + q + r = 5$; $p(D)$ and $\hat{p}(D)$ are in $R^{ABC}_{D_{1,1,1}}$ and $R^{ABC}_{D_{p,q,r}}$ respectively causing possible flip ambiguities with respect to any two lines only: AB and AC or BC and AC or AB and BC.

iv) **Group 3:** $\hat{p}(D) \in R^{ABC}_{D_{p,q,r}}$ such that p, q, $r \in \{1, 2\}$ and $p + q + r = 4$; $p(D)$ and $\hat{p}(D)$ are in $R^{ABC}_{D_{1,1,1}}$ and $R^{ABC}_{D_{p,q,r}}$ respectively causing possible flip ambiguities with respect to any one line only: AB or AC or BC.

By the definition in (14), the region $R^{ABC}_{D_{1,1,1}}$ will always be a non-empty region. If all other seven possible regions $R^{ABC}_{D_{p,q,r}}$ in (13) are null regions, then the estimated location $\hat{p}(D)$ can only be located in the unique non-empty region $R^{ABC}_{D_{1,1,1}}$, and there will be no possibility for a flipped realization. But, if there are one or more non-empty regions other than $R^{ABC}_{D_{1,1,1}}$, then the estimated location $\hat{p}(D)$ can be located in anyone of those non-empty regions, thereby creating possible flipped realization. The next section finds the probability of $\hat{p}(D)$ in each of the non-empty regions and then calculates the probability of flip ambiguities for each group defined above.

4 Derivation of Flip Ambiguity Probabilities

This section focuses on deriving analytical equations for the probability of the estimated location $\hat{p}(D)$ to be in various non-empty regions defined in Section 3.

The subsections below derived an analytical solution for the probability of flip across a single line AB. Then the derivation is extended to find the probability of flip ambiguities for all different groups.

Let the probability space containing all possible location estimates $\hat{p}(D) = (\hat{x}, \hat{y})$ be Ω, where

$$\Omega \triangleq \{\hat{p}(D) \in R_{D_1}^{AB} \cup R_{D_2}^{AB}\} \tag{16}$$

From definition (14), let us define an event set containing all possible events of $\hat{p}(D) = (\hat{x}, \hat{y})$ corresponding to the flipped realization denoted by $\zeta_{AB} \subset \Omega$ where the event that the estimated location $\hat{p}(D)$ is located in $R_{D_2}^{AB}$.

$$\zeta_{AB} = \{\hat{p}(D) \in R_{D_2}^{AB}\} \tag{17}$$

The aim is to find an expression for the probability $P(\zeta_{AB} \mid p(A), p(B), p(C), p(D))$ and then marginalize this probability over all possible locations of D to find the probability $P(\zeta_{AB} \mid p(A), p(B), p(C))$. Following the detailed analysis presented in Appendix A,

the probability $P(\zeta_{AB} \mid p(A), p(B), p(C), p(D))$ is derived as follows:

$$
\begin{aligned}
& P(\zeta_{AB} \mid p(A), p(B), p(C), p(D)) = P(\zeta'_{AB} \mid p(A), p(B), p(C), p(D)) \\
= & \int_0^{R+\overline{\epsilon}} \int_0^{R+\overline{\epsilon}} \int_0^{\min(\lambda_C, R+\overline{\epsilon})} \delta_{CD} \overline{f}(\overline{d}_{CD}) \mathrm{d}(\overline{d}_{CD}) \overline{f}(\overline{d}_{BD}) \mathrm{d}(\overline{d}_{BD}) \overline{f}(\overline{d}_{AD}) \mathrm{d}(\overline{d}_{AD}) \\
& + \int_0^{R+\overline{\epsilon}} \int_0^{R+\overline{\epsilon}} \int_{\min(\lambda_C, R+\overline{\epsilon})}^{R+\overline{\epsilon}} (1-\delta_{CD}) \overline{f}(\overline{d}_{CD}) \mathrm{d}(\overline{d}_{CD}) \overline{f}(\overline{d}_{BD}) \mathrm{d}(\overline{d}_{BD}) \overline{f}(\overline{d}_{AD}) \mathrm{d}(\overline{d}_{AD}) \\
= & \int_0^{R+\overline{\epsilon}} \int_0^{R+\overline{\epsilon}} \int_0^{R+\overline{\epsilon}} \Big((\delta_{CD} I_{CD}) + ((1-\delta_{CD})(1-I_{CD})) \Big) \overline{f}(\overline{d}_{CD}) \mathrm{d}(\overline{d}_{CD}) \overline{f}(\overline{d}_{BD}) \mathrm{d}(\overline{d}_{BD}) \overline{f}(\overline{d}_{AD}) \mathrm{d}(\overline{d}_{AD})
\end{aligned}
\tag{18}
$$

Note that the inter-sensor distances are always positive, the disc transmission model of Assumption 1 bounds the true inter-sensor distances to be $\leq R$ and the Gaussian noise model of Assumption 2 bounds the measurement errors (with 99% probability) to be $\leq \overline{\epsilon} = 3\sigma$. Thus, the inter-sensor measured distances are bounded as $0 \leq \overline{d}_{AD}$, $\overline{d}_{BD}$, $\overline{d}_{CD} \leq R + \overline{\epsilon}$, and any calculated probability is normalized by

$$
\int_0^{R+\overline{\epsilon}} \int_0^{R+\overline{\epsilon}} \int_0^{R+\overline{\epsilon}} \overline{f}(\overline{d}_{CD}) \overline{f}(\overline{d}_{BD}) \overline{f}(\overline{d}_{AD}) \mathrm{d}(\overline{d}_{CD}) \mathrm{d}(\overline{d}_{BD}) \mathrm{d}(\overline{d}_{AD}) \tag{19}
$$

Calculation of $P(\zeta_{AB} \mid p(A), p(B), p(C))$***:***

This section uses marginalization of the analytical expression (18) over all possible locations $p(D)$ to find the probability $P(\zeta_{AB} \mid p(A), p(B), p(C))$.

Using Assumption 1, sensor s_D with neighbors s_A, s_B and s_C can only be placed inside a planar region S defined by

$$
S = \left\{ p(D) : \begin{cases} \|p(D) - p(A)\| \leq R \text{ and} \\ \|p(D) - p(B)\| \leq R \text{ and} \\ \|p(D) - p(C)\| \leq R \end{cases} \right\}
$$

If the sensors are distributed uniformly over the sensor network, then the probability density function of the placement of sensor s_D for a given sensor neighborhood $s_A s_B s_C$ can be written as

$$f(p(D) \mid p(A), p(B), p(C)) = \frac{1}{A_S} \tag{20}$$

where A_S is the area of the planar region S calculated as described in Appendix B. Thus, (18) can be marginalized over all possible location $p(D)$ of the planar area S where sensor s_D can be placed, as

$$\begin{aligned} & P(\zeta_{AB} \mid p(A), p(B), p(C)) \\ &= \iint_S P(\zeta_{AB} \mid p(A), p(B), p(C), p(D)) f(D \mid p(A), p(B), p(C)) \mathrm{d}(D) \\ &= \frac{1}{A_S} \iint_S P(\zeta_{AB} \mid p(A), p(B), p(C), p(D)) \mathrm{d}(D) \end{aligned} \tag{21}$$

Defining

$$I_S(D) = \begin{cases} 1 \ D \in S \\ 0 \ otherwise \end{cases}$$

(21) can be written as

$$\begin{aligned} & P(\zeta_{AB} \mid p(A), p(B), p(C)) = \\ & \frac{1}{A_S} \iint_{\mathcal{R}^2} P(\zeta_{AB} \mid p(A), p(B), p(C), p(D)) I_S(D) \ \mathrm{d}(D) \end{aligned} \tag{22}$$

and combined with (18) to get

$$\begin{aligned} & P(\zeta_{AB} \mid p(A), p(B), p(C)) = \\ & \frac{1}{A_S} \iint_{\mathcal{R}^2} I_S(D) \int_0^{R+\overline{\epsilon}} \int_0^{R+\overline{\epsilon}} \int_0^{R+\overline{\epsilon}} \Big((\delta_{CD} I_{CD}) + ((1-\delta_{CD})(1-I_{CD})) \Big) \\ & \qquad \overline{f}(\overline{d}_{CD}) \mathrm{d}(\overline{d}_{CD}) \overline{f}(\overline{d}_{BD}) \mathrm{d}(\overline{d}_{BD}) \overline{f}(\overline{d}_{AD}) \mathrm{d}(\overline{d}_{AD}) \mathrm{d}(D) \end{aligned} \tag{23}$$

Note that appropriate changes to $I_S(D)$ will let the analysis extend to any transmission model instead of the uniform transmission model of Assumption 1.

The above analysis, without loss of generality, used the processing order of the inter sensor measurements: $\overline{d}_{AD}$, $\overline{d}_{BD}$, $\overline{d}_{CD}$. Instead, it can be used in any order with appropriate index modification. Thus, appropriate index selection of $X, Y, Z \in \{A, B, C\}$ and $X \neq Y \neq Z$ together with the above analysis will give a generalized analytical solution of the probability $P(\zeta_{XY} \mid p(A), p(B), p(C))$. A closer look at $\delta_{ZD} I_{ZD} + (1 - \delta_{ZD})(1 - I_{ZD})$, reveals that it represents a three dimensional indicator function

$$I_{\zeta_{XY}} = \begin{cases} 1 \text{ Flipped realization with respect to line } XY \\ 0 \text{ otherwise} \end{cases}$$

Thus for

$$\zeta \in \{\zeta_{XY}, \zeta_{XY} \cap \zeta_{XZ}, \zeta_{XY} \cap \zeta_{YZ}, \zeta_{XZ} \cap \zeta_{YZ}, \zeta_{XY} \cap \zeta_{XZ} \cap \zeta_{YZ}\}$$

(23) can be generalized as

$$P(\zeta \mid p(A), p(B), p(C)) = \frac{1}{A_S} \iint\limits_{\mathcal{R}^2} I_S \int\limits_0^{R+\overline{\epsilon}} \int\limits_0^{R+\overline{\epsilon}} \int\limits_0^{R+\overline{\epsilon}} I_\zeta \overline{f}(\overline{d}_{CD}) \mathrm{d}(\overline{d}_{CD}) \overline{f}(\overline{d}_{BD}) \mathrm{d}(\overline{d}_{BD}) \overline{f}(\overline{d}_{AD}) \mathrm{d}(\overline{d}_{AD}) \mathrm{d}(D) \quad (24)$$

where

$$I_{\zeta_{XY}} = \delta_{ZD} I_{ZD} + (1 - \delta_{ZD})(1 - I_{ZD})$$

$$I_{\zeta_{XY} \cap \zeta_{XZ}} = I_{\zeta_{XY}} I_{\zeta_{XZ}}$$

$$I_{\zeta_{XY} \cap \zeta_{XZ} \cap \zeta_{YZ}} = I_{\zeta_{XY}} I_{\zeta_{XZ}} I_{\zeta_{YZ}}$$

for any permutation of $X, Y, Z \in \{A, B, C\}$ and $X \neq Y \neq Z$.

The implementation of

$$P(\zeta \mid p(A), p(B), p(C), p(D)) = \int_0^{R+\overline{\epsilon}} \int_0^{R+\overline{\epsilon}} \int_0^{R+\overline{\epsilon}} I_\zeta \overline{f}(\overline{d}_{CD}) \mathrm{d}(\overline{d}_{CD}) \overline{f}(\overline{d}_{BD}) \mathrm{d}(\overline{d}_{BD}) \overline{f}(\overline{d}_{AD}) \mathrm{d}(\overline{d}_{AD}) \tag{25}$$

is given in **??**.

Note that the analytical expression (24) together with the information present in the Venn diagram (Fig. 5) help to find the conditional probabilities of Groups $0-3$ introduced in Section 3. For example, the conditional probability of Group 1 flip ambiguity can be calculated as

$$\begin{aligned} & P(Group\ 1 \mid p(A), p(B), p(C)) \\ = & P(\zeta_{AB} \cap \zeta_{AC} \cap \zeta_{BC} \mid p(A), p(B), p(C)) \end{aligned} \tag{26}$$

and the conditional probability of Group 2 flip ambiguity can be calculated as

$$\begin{aligned} & P(Group\ 2 \mid p(A), p(B), p(C)) \\ = & P(\zeta_{AB} \cap \zeta_{AC} \mid p(A), p(B), p(C)) \\ & + P(\zeta_{AB} \cap \zeta_{BC} \mid p(A), p(B), p(C)) \\ & + P(\zeta_{AC} \cap \zeta_{BC} \mid p(A), p(B), p(C)) \\ & - 2P(\zeta_{AB} \cap \zeta_{AC} \cap \zeta_{BC} \mid p(A), p(B), p(C)) \end{aligned} \tag{27}$$

5 Numerical Analysis

This section validates the correctness of the analytical solution against the flip ambiguity probabilities obtained using various simulation results.

In order to facilitate the above test, sensors with a transmission range of $10m$ are uniformly distributed over a region of $100m$ by $100m$. For a sensor network with

a large number of sensor nodes, it is reasonable to assume sensor distribution to be uniform and such assumption has been widely used in the area [4, 5, 7, 13]. Changing the sensor distribution method may only affect the frequency of collinear placement of sensor nodes. The focus of this paper is on identifying possible flip ambiguities by neighborhood geometries once the sensor nodes are placed and eliminate them from the localization process and thus, this numerical analysis only consider uniformly distributed sensor networks to demonstrate the correctness of the analytical solution.

If the true distance $\mid p(Y) - p(X) \mid$ between any two nodes s_Y and s_X is smaller than the transmission range R, then the nodes are set to be neighbors. A Gaussian noise satisfying Assumption 2 and with a mean of zero and variance σ^2, where σ varies from $0.1m$ to $0.5m$, is used to blur the true inter-sensor distances to represent the measured inter-sensor distances as in (1). FCQs for the comparisons are selected from a pool of 4-node subnetworks of the above network.

Since all the generalized equations of the probabilities are built upon the probability analysis of $P(\zeta_{AB} \mid p(A), p(B), p(C), p(D))$ and $P(\zeta_{AB} \mid p(A), p(B), p(C))$, only the results of $P(\zeta_{AB} \mid p(A), p(B), p(C), p(D))$ and $P(\zeta_{AB} \mid p(A), p(B), p(C))$ with respect to arbitrarily placed sensor neighborhoods are presented in this section.

Denote the probabilities $P(\zeta_{AB} \mid p(A), p(B), p(C), p(D))$ and $P(\zeta_{AB} \mid p(A), p(B), p(C))$ obtained via simulations as $P_S(\zeta_{AB} \mid A, B, C, D)$ and $P_S(\zeta_{AB} \mid A, B, C)$, and via the analytical results as $P_A(\zeta_{AB} \mid A, B, C, D)$ and $P_A(\zeta_{AB} \mid A, B, C)$ respectively. Define the average difference between the analytical and simulated flip ambiguity probabilities as,

$$\Delta_1 = \frac{\sum\limits_{N_t} \mid P_S(\zeta_{AB} \mid A, B, C, D) - P_A(\zeta_{AB} \mid A, B, C, D) \mid}{N_t} \tag{28}$$

$$\Delta_2 = \frac{\sum_{N_t} \mid P_S(\zeta_{AB} \mid A,B,C) - P_A(\zeta_{AB} \mid A,B,C) \mid}{N_t} \tag{29}$$

where $N_t = 1000$ is the number of FCQs used in the calculation of the probability of flip ambiguities.

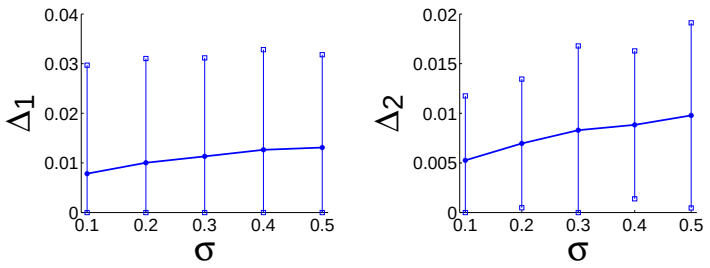

(a) Results of (28) (b) Results of (29)

Fig. 6 Comparison of the simulation results $P_S(\zeta_{AB} \mid A,B,C,D)$ and $P_S(\zeta_{AB} \mid A,B,C)$ with the results obtained using the analytical expressions $P_A(\zeta_{AB} \mid A,B,C,D)$ and $P_A(\zeta_{AB} \mid A,B,C)$ respectively for different values of σ. The vertical line segments represent the standard error bars of Δ_1 and Δ_2.

Fig. 6(a) and (b) respectively show the deviation of Δ_1 and Δ_2 with respect to σ. *From both results it can be seen that the derived analytical expressions of the probabilities match with the probability of flip ambiguity accurately.*

6 Substantial and Negligible Flip Ambiguities

In the previous analysis, a location estimate $\hat{p}(D)$ is considered a flipped realization with respect to the line XY when the location estimate $\hat{p}(D)$ and the true location $p(D)$ of the sensor s_D are on different sides of the line XY, where XY is the line joining any two neighbors $s_X, s_Y \in \{s_A, s_B, s_C\}$. But not all such flipped realizations may cause large estimation errors.

The generic task of sensor localization is to estimate the location of each sensor such that the magnitude of the corresponding estimation error is less than or equal to a predefined accuracy level $\delta_S > 0$, when the corresponding absolute measurement errors are less than a predefined error bound $\overline{\epsilon} > 0$. Hence an error caused by a flip ambiguity where $\|p(D) - \hat{p}(D)\| < \delta_S$ is not substantial in terms of the localization task. To take this observation into consideration, a *substantial flip ambiguity* is defined as a flip ambiguity where the distance between the true location $p(D)$ and the possible location estimate $\hat{p}(D)$ is at least δ_S. A flip ambiguity which is not a substantial flip ambiguity is called a *negligible flip ambiguity*.

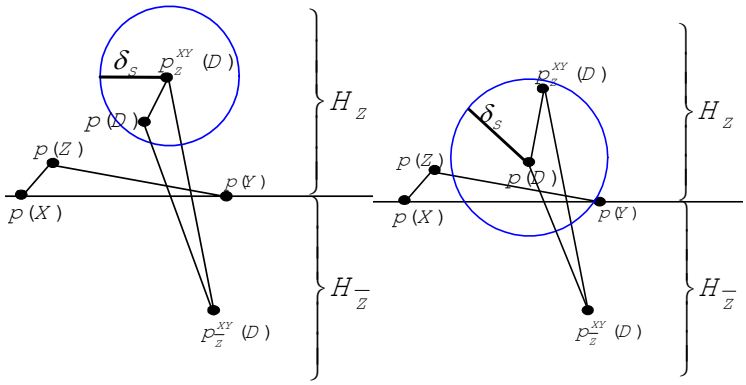

Fig. 7 Comparison of $\|p(D) - p_Z^{XY}(D)\|$, $\|p(D) - p_{\overline{Z}}^{XY}(D)\|$ and $\|p_Z^{XY}(D) - p_{\overline{Z}}^{XY}(D)\|$ with respect to δ_S.

In a localization problem with two possible location estimates $p_Z^{XY}(D) \in H_Z$ and $p_{\overline{Z}}^{XY}(D) \in H_{\overline{Z}}$ as in Fig 7, (see Section 4 and Fig. 6 for details of notions) $p_Z^{XY}(D)$ can be treated as the correct location estimate and $p_{\overline{Z}}^{XY}(D)$ as the flipped location estimate.

In a localization case with flip ambiguity, the smallest and largest possible estimation errors are defined by the smallest and largest distances between two points one of which is in $R_{D_1}^{XY}$ and the other in $R_{D_2}^{XY}$ (see Fig.8). Therefore, flip ambiguity is substantial if

$$\|p_Z^{XY}(D) - p_{\overline{Z}}^{XY}(D)\| \geq \delta_S + 4\overline{\epsilon} \tag{30}$$

and is negligible if

$$\|p_Z^{XY}(D) - p_{\overline{Z}}^{XY}(D)\| < \delta_S + 4\overline{\epsilon} \tag{31}$$

(31) directly implies the following result:

Proposition 1 *Assume that $\delta_S \geq 8\overline{\epsilon}$, then for any case where $R_{D_1}^{XY}$ and $R_{D_2}^{XY}$ are joint, the flip ambiguity is negligible.*

Proposition 1 implies that a substantial flip ambiguity occurs only when the regions $R_{D_1}^{XY}$ and $R_{D_2}^{XY}$ are disjoint as in Fig. 8. With this information, all groups of flip ambiguities defined in the Venn Diagram (Fig. 5) are analyzed below to see which groups are subject to substantial flip ambiguities and which groups are not.

In Group 2 and Group 3 flip ambiguities, the estimated location do not flip across at least one line $XY \in \{AB, AC, BC\}$. When the estimated location does not flip across a line XY, using definition in (14), it can be stated that the true location $p(D)$ and the estimated location $\hat{p}(D)$ both lie inside $R_{D_1}^{XY}$ with respect to the line XY as shown in Fig. 8. In Assumption 2, if the threshold value $\overline{\epsilon}$ is considered small, then the non-empty region $R_{D_1}^{XY}$ can be approximated by a square of side $2\overline{\epsilon}$ (see Fig. 8). Thus, the maximum distance between the true location $p(D)$ and the estimated location $\hat{p}(D)$ can only be the diagonal length $2\sqrt{2}\overline{\epsilon}$ of the square. For a predefined measurement error threshold $\overline{\epsilon}$, it is reasonable to predefine a location estimation accuracy level $\delta_s > 2\sqrt{2}\overline{\epsilon}$.

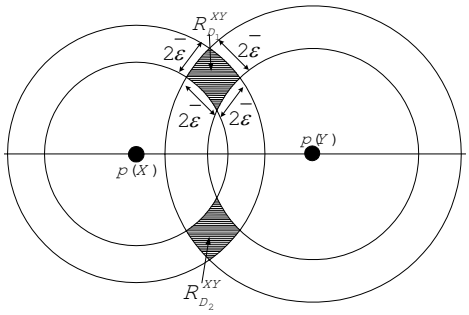

Fig. 8 Illustration of disjoint regions $R_{D_1}^{XY}$ and $R_{D_2}^{XY}$.

Even without this approximation, it can be easily shown that the distance between $p(D)$ and $\hat{p}(D)$ needs to be less than $4\overline{\epsilon}$, which is comparable to the measurement error. Thus, Group 2 and Group 3 flip ambiguities in a localization task can be treated as negligible flip ambiguities, and the only substantial flip ambiguity need to be considered in a localization task is the Group 3 flip ambiguities when $R_{D_1}^{XY}$, $R_{D_2}^{XY}$ are disjoint for all $p(X), p(Y) \in \{p(A), p(B), p(C)\}$.

7 Performance Enhancement of Localization Algorithms Using the Flip Ambiguity Probability

Large number of tiny sensors are randomly distributed over large regular shaped areas in applications like bushfire surveillance, water quality surveillance and precision irrigation and are stationary after being deployed. In such networks, a sequential algorithm is sufficient and thus the performance enhancement of sequential localization algorithm using the probability of flip ambiguity calculated via (26) is presented in this section.

A sequential localization algorithm performing in an iterative manner is considered where at each iteration all sensors with unknown location which have three or more neighbors with known location information are localized. These location known

neighbors can either be anchors or some sensors defining a local coordinate system. When a sensor get localized, it is elevated to anchor status, thereby increasing the chances of the other sensors with unknown location being localized in the subsequent iterations [7–11].

Simulations: To evaluate the performance enhancement using the derived flip ambiguity expressions, we have performed a sequence of simulations deploying 100 different simulated sensor networks, in which different random seeds are used to uniformly distribute 100 sensors in each sensor network covering a region of $100m$ by $100m$. Ten percent of these sensors are randomly selected and designated as anchors.

The inter-sensor measured distances between neighboring nodes are obtained using (1) and Assumptions 1, 2, where σ is chosen as $0.2m$. The location of the sensors with unknown locations are estimated by minimizing the cost function (A.2).

In the simulations, the transmission range of the sensor network is adjusted while keeping the number of the sensors fixed, in order to vary the average node degree between $4-25$. The average mean squared error in location estimates is calculated and normalized to the transmission range R as:

$$MSE = \frac{1}{|\{n|V_n \neq \emptyset\}|} \sum_{\substack{n=1 \\ |V_n|\neq 0}}^{50} \frac{1}{|V_n|} \frac{\sum_{i\in V_n} (x_i - \hat{x}_i)^2 + (y_i - \hat{y}_i)^2}{R^2}$$

where $(\hat{x}_i, \hat{y}_i)$ and (x_i, y_i) are respectively the estimated and true location of sensor i, V_n is the set of nodes localized in the n^{th} sensor network, and $|V_n|$ is the number of nodes in V_n.

The traditional sequential localization algorithms [7–11] uses any FCQ to do trilateration. Instead, this paper uses the analytically calculated probability of flip ambiguity to select the robust FCQ that does not suffer from flip ambiguity problems. To com-

pare different scenarios, sensor networks are simulated in two different ways, where FCQs with $A, B, C \in N_X$ and X are chosen differently as described below:

Case 1: i Any FCQ.

ii Any FCQ with probability of flip less than 40%.

iii Any FCQ with probability of flip less than 25%.

iv Any FCQ with probability of flip less than 15%.

v Any FCQ with probability of flip less than 7%.

vi Most robust FCQ by criterion [6]

vii Most robust FCQ by criterion in [4].

Case 2: i Any FCQ.

ii Most robust FCQ with probability of flip less than 40%.

iii Most robust FCQ with probability of flip less than 25%.

iv Most robust FCQ with probability of flip less than 15%.

v Most robust FCQ with probability of flip less than 7%.

vi Most robust by criterion [6]

vii Most robust by criterion in [4].

Simulation results of Case 1 and Case 2 are shown in Fig. 9 and Fig. 10 respectively. From these figures, it can be seen that average numbers of localized nodes as well as the average estimation error decrease as the neighbor selection method move from (i) to (vii). This clearly indicates that when the threshold of acceptable probability of flip ambiguity is relaxed, the number of localized nodes is increasing, however due to more miss-detected flipped realization the average estimation error is increasing as well. The figures also clearly show that the average estimation error is much smaller in Case 2 than in Case 1 due to the selection of the most robust FCQ for the localization process.

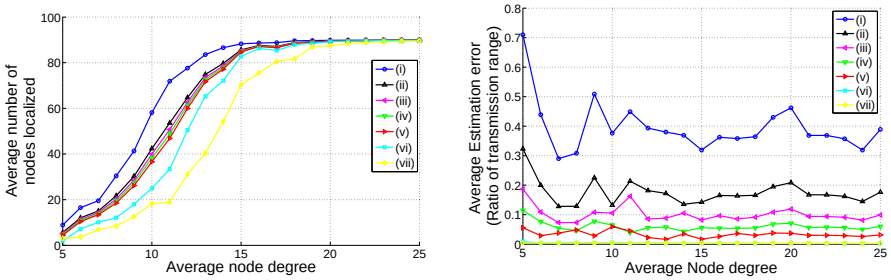

(a) (b)

Fig. 9 Performance of different neighbor selection methods (i) to (vii) in Case 1 simulations. (a) Average nodes localized. (b) Average estimation error

This can be explained by the fact that Case 1 is based on random choices of an FCQ each time from the group of FCQs with a probability of flip ambiguity less than the given threshold, while Case 2 uses the most robust FCQ from the same group of FCQs with a probability of flip ambiguity less than the given threshold.

An efficient robustness check must be able to detect as many flip ambiguities as possible while making as few false alarms as possible. From these aspects, the above simulation results demonstrate that by choosing a suitable threshold value for (24), the localization performance can be optimized using a flip ambiguity detection criterion

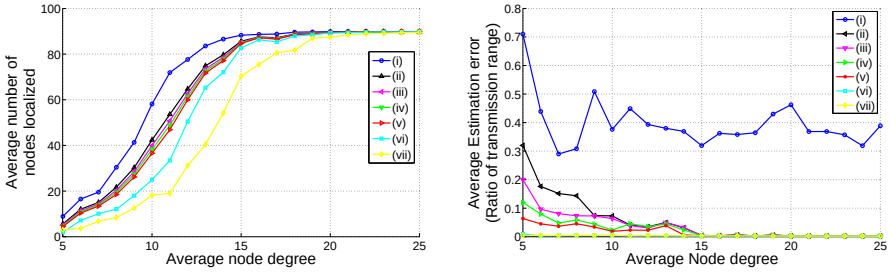

(a) (b)

Fig. 10 Performance of different neighbor selection methods (i) to (vii) in Case 2 simulations. (a) Average nodes localized. (b) Average estimation error

based on (25), and a performance better than [4,6] in terms of the nodes localized, yet having a comparable performance in terms of average estimation error.

8 Conclusion and Future Work

The co-authors of this paper have well demonstrated in a recent work [6, 16] that the identification of the likelihood of flip ambiguities in location estimates and rectification of such flip ambiguities from the localization process enhance the performance of localization algorithm significantly.

To help such identification and rectification tasks, an analytical expression to calculate the probability of flip ambiguities in an arbitrary neighborhood $s_A s_B s_C$ is presented in this paper. This probability can be used to improve the performance of localization algorithms either by using it to eliminate neighborhoods from the localization process which are likely to cause flip ambiguity or by using it to assign confidence factors reflecting the likelihood of flip ambiguities associated with the location estimates.

The simulations show that the probability of flip ambiguity calculated using the analytical expression derived in the paper for the flip ambiguity probability for a given node neighborhood, i.e. FCQ, matches accurately with the probability of flip ambiguity obtained using simulation. This paper has also demonstrated performance enhancement of localization algorithms via the usage of the analytical expression derived in the paper for the flip ambiguity probability for a given node neighborhood, i.e. FCQ, on elimination of flip ambiguities in the localization process.

As a future work, confidence factors can be calculated using the analytical expression derived in the paper for the flip ambiguity probability for a given node neighbor-

hood, i.e. FCQ, and reflecting the likelihood of flip ambiguities of each location estimate can be incorporated with the localization algorithms to enhance the performance.

A Calculation of $P(\zeta_{AB} \mid p(A), p(B), p(C), p(D))$

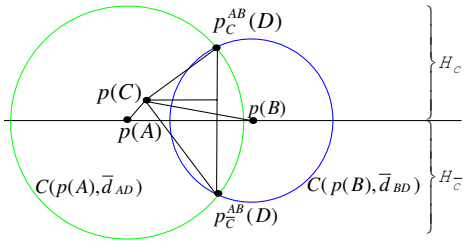

Fig. A.1 Division of the plane into two open halves H_C and $H_{\overline{C}}$ with respect to the three known neighbor locations $p(A)$, $p(B)$ and $p(C)$.

Denote by H_C the open half plane containing the sensor s_C, bordered by the line AB as shown in Fig. A.1, then the complementary half plane on the other side of line AB can be denoted by $H_{\overline{C}}$. For a non-collinear neighborhood $N_D = \{s_A, s_B, s_C\}$, H_C and $H_{\overline{C}}$ are well defined. Denote by $p_C^{AB}(D)$ and $p_{\overline{C}}^{AB}(D)$ the intersection points of the two circles $\mathcal{C}(p(A), \overline{d}_{AD})$ and $\mathcal{C}(p(B), \overline{d}_{BD})$. Without loss of generality, let $p_C^{AB}(D) \in H_C$, which will leave the other intersection point $p_{\overline{C}}^{AB}(D) \in H_{\overline{C}}$ as shown in Fig. A.1.

When considering distance measurements from only two neighboring sensors s_A and s_B, both points $p_C^{AB}(D)$ and $p_{\overline{C}}^{AB}(D)$ are possible candidates for the location estimate $\hat{p}(D)$ of sensor s_D with $(\|p(A) - \hat{p}(D)\| - \overline{d}_{AD})^2 + (\|p(B) - \hat{p}(D)\| - \overline{d}_{BD})^2 = 0$. When the third distance measurement from the neighboring sensor s_C is included in the localization process, a new candidate for the location estimate $\hat{p}(D)$ considering the third distance measurement $\overline{d}_{CD}$ is obtained as

$$\hat{p}(D) \triangleq \arg \min_{\hat{p}^*(D) \in R_D^{AB}} J(\hat{p}^*(D)) \tag{A.1}$$

where the cost function $J(\hat{p}^*(D))$ is defined as

$$\begin{aligned} J(\hat{p}^*(D)) \triangleq & (\|p(A) - \hat{p}^*(D)\| - \overline{d}_{AD})^2 \\ & + (\|p(B) - \hat{p}^*(D)\| - \overline{d}_{BD})^2 \\ & + (\|p(C) - \hat{p}^*(D)\| - \overline{d}_{CD})^2 \end{aligned} \tag{A.2}$$

Proposition A.1 *With non-collinear neighbors s_A, s_B, s_C, the location estimate $\hat{p}(D)$ satisfies the following:*

i $\hat{p}(D) \in H_C$ *if* $0 \leq \overline{d}_{CD} < \lambda_C - 2\overline{\epsilon}$

ii $\hat{p}(D) \in H_{\overline{C}}$ *if* $\lambda_C + 2\overline{\epsilon} < \overline{d}_{CD} \leq R + \overline{\epsilon}$

where $\lambda_C = \frac{\|p(C) - p_C^{AB}(D)\| + \|p(C) - p_{\overline{C}}^{AB}(D)\|}{2}$.

Proof: Because of Assumption 2, we have (i) $D \in R_D^{AB} = R_{D_1}^{AB} \cup R_{D_2}^{AB}$ and (ii) D lies in the annulus with center C and radii $\overline{d}_{CD} \pm \overline{\epsilon}$. Denote the intersection regions of this annulus with $R_D^{AB} \cap H_C$ and $R_D^{AB} \cap H_{\overline{C}}$ by S_{C_1} and $S_{\overline{C}_1}$ respectively; and the reflections of S_{C_1} and $S_{\overline{C}_1}$ with respect to AB by $S_{\overline{C}_2}$ and S_{C_2} respectively. Let $S_C = S_{C_1} \cup S_{C_2}$ and $S_{\overline{C}} = S_{\overline{C}_1} \cup S_{\overline{C}_2}$. Note that $S_C \subset R_D^{AB} \cap H_C$ and $S_{\overline{C}} \subset R_D^{AB} \cap H_{\overline{C}}$ and that neither S_C nor $S_{\overline{C}}$ is empty set since each of them contains either D or the reflection of D with respect to AB. The value of $\hat{p}^*(D)$ minimizing (A.1) lies in either S_C or $S_{\overline{C}}$ since (i) at least one of the three quadratic components of $J(\hat{p}^*(D))$ is larger than $\overline{\epsilon}^2$ and hence $J(\hat{p}^*(D)) > \overline{\epsilon}^2$ outside $S_C \cup S_{\overline{C}}$ and (ii) $S_C \cup S_{\overline{C}}$ contains points $\hat{p}^*(D)$ at which $J(\hat{p}^*(D)) \leq \overline{\epsilon}^2$ (the intersection points of the circles $\mathcal{C}(A, \overline{d}_{AD})$, $\mathcal{C}(B, \overline{d}_{BD})$, $\mathcal{C}(C, \overline{d}_{CD})$).

First consider the case $0 \leq \overline{d}_{CD} < \lambda_C - 2\overline{\epsilon}$. Noting that $\|p(C) - p_C^{AB}(D)\| < \lambda_C < \|p(C) - p_{\overline{C}}^{AB}(D)\|$ and analyzing all possible values of $\overline{d}_{CD} < \lambda_C - 2\overline{\epsilon}$, it can be established that

$$|\|p(C) - p_C^{AB}(D)\| - \overline{d}_{CD}| < |\|p(C) - p_{\overline{C}}^{AB}(D)\| - \overline{d}_{CD}| - 4\overline{\epsilon} \tag{A.3}$$

For each point $\hat{p}^*(D) \in S_{\overline{C}}$, the reflection $\hat{p}_2^*(D) \in S_C$ of $\hat{p}^*(D)$ with respect to AB satisfies

$$\|p(A) - \hat{p}^*(D)\| = \|p(A) - \hat{p}_2^*(D)\|$$

$$\|p(B) - \hat{p}^*(D)\| = \|p(B) - \hat{p}_2^*(D)\|$$

Hence we have

$$\begin{aligned} & J(\hat{p}^*(D)) - J(\hat{p}_2^*(D)) \\ & = (\|p(C) - \hat{p}^*(D)\| - \overline{d}_{CD})^2 - (\|p(C) - \hat{p}_2^*(D)\| - \overline{d}_{CD})^2 \end{aligned} \tag{A.4}$$

Furthermore, since $\hat{p}^*(D) \in S_{\overline{C}} \subset R_D^{AB} \cap H_{\overline{C}}$ and $\hat{p}_2^*(D) \in S_C \subset R_D^{AB} \cap H_C$, we have

$$|\|p(C) - \hat{p}^*(D)\| - \|p(C) - p_{\overline{C}}^{AB}(D)\|| \leq 2\overline{\epsilon}$$

$$|\|p(C) - \hat{p}_2^*(D)\| - \|p(C) - p_C^{AB}(D)\|| \leq 2\overline{\epsilon}$$

which, respectively imply

$$|\|p(C) - \hat{p}^*(D)\| - \overline{d}_{CD}| \geq |\|p(C) - p_{\overline{C}}^{AB}(D)\| - \overline{d}_{CD}| - 2\overline{\epsilon} \tag{A.5}$$

$$|\|p(C) - \hat{p}_2^*(D)\| - \overline{d}_{CD}| \leq |\|p(C) - p_C^{AB}(D)\| - \overline{d}_{CD}| + 2\overline{\epsilon} \tag{A.6}$$

Combining (A.5), (A.6) with (A.3) we obtain

$$|\|p(C) - \hat{p}_2^*(D)\| - \overline{d}_{CD}| < |\|p(C) - \hat{p}^*(D)\| - \overline{d}_{CD}| \tag{A.7}$$

(A.4) and (A.7) imply that $\hat{p}(D)$ cannot be in $H_{\overline{C}}$, i.e. $\hat{p}(D) \in H_C$.

The case $\lambda_C + 2\overline{\epsilon} < \overline{d}_{CD} \leq R + \overline{\epsilon}$ can be analysed similarly to obtain that in this case $\hat{p}(D) \in H_{\overline{C}}$. This completes the proof of Proposition A.1.

In (14), it is defined that $p(D) \in R_{D_1}^{AB}$ and, thus, a flipped realization occurs when

i $\hat{p}(D) \in H_C$ and $R_{D_1}^{AB} \subset H_{\overline{C}}$

ii $\hat{p}(D) \in H_{\overline{C}}$ and $R_{D_1}^{AB} \subset H_C$

With this information, two support spaces can be defined for the events defined in (16) and (17) as:

$$\begin{aligned} \Omega' &= \{\hat{p}(D) \in H_C \cup H_{\overline{C}}\} \\ &\triangleq \{\overline{d}_{AD}, \overline{d}_{BD}, \overline{d}_{CD} \in [0, R + \overline{\epsilon}] \mid p(A), p(B), p(C), p(D)\} \end{aligned} \tag{A.8}$$

$$\zeta'_{AB} = \begin{cases} \{\hat{p}(D) \in H_C\} \text{ when } R_{D_1}^{AB} \subset H_{\overline{C}} \\ \{\hat{p}(D) \in H_{\overline{C}}\} \text{when } R_{D_1}^{AB} \subset H_C \end{cases} \tag{A.9}$$

Using Proposition A.1 and assuming that $\overline{\epsilon}$ is sufficiently small, (A.9) can be approximated by

$$\zeta'_{AB} \cong \begin{cases} \{\overline{d}_{AD}, \overline{d}_{BD} \in [0, R+\overline{\epsilon}], \\ \qquad \overline{d}_{CD} \in [0, \lambda_C] \mid p(A), p(B), p(C), p(D)\} \\ \qquad\qquad \text{when } R^{AB}_{D_1} \subset H_{\overline{C}} \\ \\ \{\overline{d}_{AD}, \overline{d}_{BD} \in [0, R+\overline{\epsilon}], \\ \qquad \overline{d}_{CD} \in [\lambda_C, R+\overline{\epsilon}] \mid p(A), p(B), p(C), p(D)\} \\ \qquad\qquad \text{when } R^{AB}_{D_1} \subset H_C \end{cases} \tag{A.10}$$

The measured distances $\overline{d}_{AD}$, $\overline{d}_{BD}$ and $\overline{d}_{CD}$ are respectively the true distances $\|p(A) - p(D)\|$, $\|p(B) - p(D)\|$ and $\|p(C) - p(D)\|$ blurred by additive Gaussian measurement errors $\mathcal{N}(0, \sigma^2)$ as in (1). Thus, the probability density functions $f(\overline{d}_{AD} \mid p(A), p(B), p(C), p(D))$, $f(\overline{d}_{BD} \mid p(A), p(B), p(C), p(D))$ and $f(\overline{d}_{CD} \mid p(A), p(B), p(C), p(D))$ of the measured distances $\overline{d}_{AD}$, $\overline{d}_{BD}$ and $\overline{d}_{CD}$ can be written as

$$\begin{aligned} f(\overline{d}_{AD} \mid p(A), p(B), p(C), p(D)) &= f(\overline{d}_{AD} \mid p(A), p(D)) \\ &= \mathcal{N}(\|p(A) - p(D)\|, \sigma^2) \end{aligned}$$

$$\begin{aligned} f(\overline{d}_{BD} \mid p(A), p(B), p(C), p(D)) &= f(\overline{d}_{BD} \mid p(B), p(D)) \\ &= \mathcal{N}(\|p(B) - p(D)\|, \sigma^2) \end{aligned}$$

$$\begin{aligned} f(\overline{d}_{CD} \mid p(A), p(B), p(C), p(D)) &= f(\overline{d}_{CD} \mid p(C), p(D)) \\ &= \mathcal{N}(\|p(C) - p(D)\|, \sigma^2) \end{aligned} \tag{A.11}$$

and are independent of each other. In order to keep the equations simple, the probability density functions are re-named as follows:

$$\overline{f}(\overline{d}_{AD}) \triangleq f(\overline{d}_{AD} \mid p(A), p(B), p(C), p(D))$$
$$\overline{f}(\overline{d}_{BD}) \triangleq f(\overline{d}_{BD} \mid p(A), p(B), p(C), p(D))$$
$$\overline{f}(\overline{d}_{CD}) \triangleq f(\overline{d}_{CD} \mid p(A), p(B), p(C), p(D))$$

Due to the independent nature of the probability density functions $\overline{f}(\overline{d}_{AD})$, $\overline{f}(\overline{d}_{BD})$ and $\overline{f}(\overline{d}_{CD})$, define two binary functions δ_{CD} and I_{CD} as

$$\delta_{CD} = \begin{cases} 1 \text{ If } R_{D_1}^{AB} \subset H_{\overline{C}} \\ 0 \text{ If } R_{D_1}^{AB} \subset H_C \end{cases}$$

$$I_{CD} = \begin{cases} 1 \text{ If } \overline{d}_{CD} \in [0, \min(\lambda_C, R)] \\ 0 \text{ Otherwise} \end{cases}$$

which let the probability $P(\zeta_{AB} \mid p(A), p(B), p(C), p(D))$ to be expressed as

$$\begin{aligned}
&P(\zeta_{AB} \mid p(A), p(B), p(C), p(D)) = P(\zeta'_{AB} \mid p(A), p(B), p(C), p(D)) \\
&= \int_0^{R+\overline{\epsilon}} \int_0^{R+\overline{\epsilon}} \int_0^{\min(\lambda_C, R+\overline{\epsilon})} \delta_{CD} \overline{f}(\overline{d}_{CD}) \mathrm{d}(\overline{d}_{CD}) \overline{f}(\overline{d}_{BD}) \mathrm{d}(\overline{d}_{BD}) \overline{f}(\overline{d}_{AD}) \mathrm{d}(\overline{d}_{AD}) \\
&\quad + \int_0^{R+\overline{\epsilon}} \int_0^{R+\overline{\epsilon}} \int_{\min(\lambda_C, R+\overline{\epsilon})}^{R+\overline{\epsilon}} (1-\delta_{CD}) \overline{f}(\overline{d}_{CD}) \mathrm{d}(\overline{d}_{CD}) \overline{f}(\overline{d}_{BD}) \mathrm{d}(\overline{d}_{BD}) \overline{f}(\overline{d}_{AD}) \mathrm{d}(\overline{d}_{AD}) \\
&= \int_0^{R+\overline{\epsilon}} \int_0^{R+\overline{\epsilon}} \int_0^{R+\overline{\epsilon}} \Big((\delta_{CD} I_{CD}) + ((1-\delta_{CD})(1-I_{CD})) \Big) \overline{f}(\overline{d}_{CD}) \mathrm{d}(\overline{d}_{CD}) \overline{f}(\overline{d}_{BD}) \mathrm{d}(\overline{d}_{BD}) \overline{f}(\overline{d}_{AD}) \mathrm{d}(\overline{d}_{AD})
\end{aligned} \tag{A.12}$$

B Calculation of A_S

The neighbor geometry $p(A)p(B)p(C)$ and the transmission range R determines the area A_S where the sensor s_D could be placed. The possible neighbor geometry $p(A)p(B)p(C)$ could be divided into two groups as shown in Fig. B.1. The following calculation of A_S considered the neighbor geometries $p(A)p(B)p(C)$ in the group $\|p(C) - P_1\| < R$. The same argument can be applied to the neighbor geometries $p(A)p(B)p(C)$ in the other group $\|p(C) - P_1\| \geq R$. The

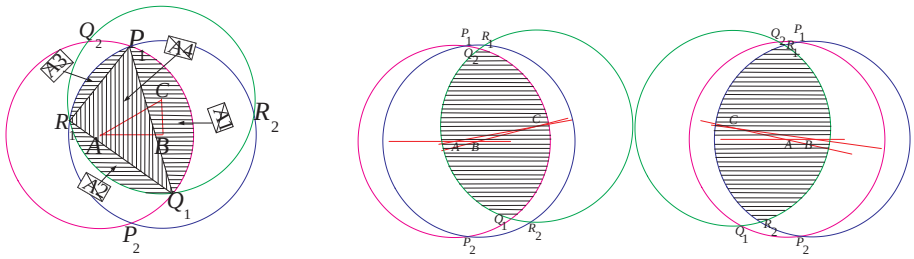

(a) $\|C - P_1\| < R$ (b) $\|C - P_1\| \geq R$

Fig. B.1 The area in which sensor s_D can be placed such that D is a neighbor to all three sensors s_A, s_B and s_C. Here P_1 and P_2 are the intersection points of circles $\mathcal{C}'(p(A), R)$ with center $p(A)$ and radius R and $\mathcal{C}'(p(B), R)$ with center $p(B)$ and radius R.

area A_S for placement of sensor s_D can be divided into three circle segments and a triangle as illustrated in the Fig. B.1(a) and calculated as

(i) A_1=area of segment P_1Q_1

$= R^2 \sin^{-1} \frac{\|P_1 - Q_1\|}{2R} - \frac{R^2}{2} \sin(2 \sin^{-1} \frac{\|P_1 - Q_1\|}{2R})$

(ii) A_2=area of segment Q_1R_1

$= R^2 \sin^{-1} \frac{\|Q_1 - R_1\|}{2R} - \frac{R^2}{2} \sin(2 \sin^{-1} \frac{\|Q_1 - R_1\|}{2R})$

(iii) A_3=area of segment P_1R_1

$= R^2 \sin^{-1} \frac{\|P_1 - R_1\|}{2R} - \frac{R^2}{2} \sin(2 \sin^{-1} \frac{\|P_1 - R_1\|}{2R})$

(iv) A_4=area of $\triangle P_1Q_1R_1$

$= \sqrt{s(s - \|P_1 - Q_1\|)(s - \|Q_1 - R_1\|)(s - \|P_1 - R_1\|)}$

where $s = \frac{\|P_1 - Q_1\| + \|Q_1 - R_1\| + \|P_1 - R_1\|}{2}$

Thus the possible area for placement of D

$$A_S = A_1 + A_2 + A_3 + A_4 \tag{B.1}$$

References

1. T. Eren, D. Goldenberg, W. Whiteley, Y. Yang, A. Morse, B. Anderson, and P. Belhuneur, "Rigidity, computation, and randomization in network localisation," in *IEEE INFOCOM*, vol. 4, 2004, pp. 2673 – 2684.

2. D. Goldenberg, A. Krishnamurthy, W. Maness, Y. Yang, and A. Young, "Network localization in partially localizable networks," in *IEEE INFOCOM*, 2005, pp. 313 – 326.

3. B. Hendrickson, "Conditions for unique graph realizations," *SIAM J. Comput.*, vol. 21, no. 1, pp. 65 – 84, 1992.

4. D. Moore, J. Leonard, D. Rus, and S. Teller, "Robust distributed network localization with noisy range measurements," in *2nd ACM Conf. on Embedded Networked Sensor Systems*, 2004, pp. 50 – 61.

5. G. Mao, B. Fidan, and B. Anderson, "Wireless sensor network localization techniques," *Computer Networks*, vol. 51, no. 10, pp. 2529 – 2553, 2007.

6. A.A. Kannan, B. Fidan, and G. Mao, "Robust distributed sensor network localization based on analysis of flip ambiguities," in *IEEE GlobeCom*, 2008, pp. 1 – 6.

7. D. Niculescu and B. Nath, "Dv based positioning in ad hoc networks," *Telecommunication Systems*, vol. 22, no. 1-4, pp. 267 – 280, 2003.

8. A. Savvides, C. C. Han, and M. B. Srivastava, "Dynamic fine-grained localization in ad-hoc networks of sensors," in *ACM SigMobile*, 2001, pp. 166 – 179.

9. C. Savarese and J. Rabaey, "Robust positioning algorithms for distributed ad-hoc wireless sensor networks," in *Proceedings of the General Track: 2002 USENIX Annual Technical Conference*, 2002, pp. 317 – 327.

10. C. Savarese, J. Rabaey, and J. Beutel, "Locationing in distributed ad-hoc wireless sensor networks," in *ICASSP*, 2001, pp. 2037 – 2040.

11. L. Meertens and S. Fitzpatrick, "The distributed construction of a global coordinate system in a network of static computational nodes rom inter-node distances," Kestrel Institute, formal report KES.U.04.04, 2004.

12. S. Capkun, M. Hamdi, and J. Hubaux, "Gps-free positioning in mobile ad-hoc networks," in *34th Hawaii International Conference on System Sciences*, 2001, pp. 3481 – 3490.

13. X. Ji and H. Zha, "Sensor positioning in wireless ad-hoc sensor networks using multidimensional scaling," in *IEEE INFOCOM*, vol. 4, 2004, pp. 2652 – 2661.

14. Y. Kwon, K. Mechitov, S. Sundresh, W. Kim, and G. Agha, "Resilient localization for sensor networks in outdoor environments," in *IEEE ICDCS*, 2005, pp. 643 – 652.

15. A. Kannan, G. Mao, and B. Vucetic, "Simulated annealing based wireless sensor network localization with flip ambiguity mitigation," in *IEEE Vehicular Technology Conference*, vol. 2, 2006, pp. 1022 — 1026.

16. A.A. Kannan, B. Fidan and G. Mao, "Analysis of flip ambiguities for robust sensor network localization," in *IEEE Transactions on Vehicular Technology*, Vol 59, No. 4, 2010, pp. 2057 – 2070.

17. A. T. Ihler, J. W. Fisher, III, R. L. Moses, and A. S. Willsky, "Nonparametric belief propagation for self-localization of sensor networks," in *IEEE Journal on Selected Areas in Communications*, vol. 23, 2005, pp. 809 – 819.

18. S. Lederer, Y. Wang, and J. Gao, "Connectivity-based localization of large scale sensor networks with complex shape," in *IEEE INFOCOM*, 2008, pp. 789 – 797.

19. J. Fang, M. Cao, A. Morse, and B. Anderson, "Localization of sensor networks using sweeps," in *IEEE Conference on Decision and Control*, 2006, pp. 4645 — 4650.

20. Y. Wang, S. Lederer, and J. Gao, "Connectivity-based sensor network localization with incremental delaunay refinement method," in *IEEE INFOCOM*, 2009, pp. 2401 — 2409.

21. Z. Yang, Y. Liu, and X. Li, "Beyond trilateration: On the localizability of wireless ad-hoc networks," in *IEEE INFOCOM*, 2009, pp. 2392 — 2400.

22. F. Sittile and M. Spirito, "Robust localization for wireless sensor networks," in *IEEE SECON*, 2008, pp. 46 – 54.

23. A. Kannan, B. Fidan, G. Mao, and B. Anderson, "Analysis of flip ambiguities in distributed network localization," in *Information, Decision and Control*, 2007, pp. 193 – 198.

24. D. Goldenberg, P. Bihler, M. Cao, J. Fang, B. Anderson, A. Morse, and Y. Yang, "Localization in sparse networks using sweeps," in *ACM/IEEE MobiCom*, 2006, pp. 110 – 121.

25. N. Patwari, A. Hero III, M. Perkins, S. Neiyer, and R. ODea, "Relative location estimation in wireless sensor networks," *IEEE Transactions on Signal Processing*, vol. 51, no. 8, pp. 2137 — 2148, 2003.

26. A. Kannan, B. Fidan, and G. Mao, "Implementation of the Generic Equation (25) on the Journal Paper *Use of Flip Ambiguity Probabilities in Robust Sensor Network Localization*," in `http://www.ee.usyd.edu.au/~guoqiang/publication`